A Preliminary Study of Trimarans

Alexander W. Gray
School Address: West Virginia University
College of Engineering and Mineral Resources
P.O. Box 6070
Morgantown, WV 26506-6070
agray1@mix.wvu.edu
Home Address: 3909 Autumn Dr.
Huron, Oh 44839
mobulidaex@gmail.com

Mentor: Dr. Z. Zong
School of Naval Architecture
Dalian University of Technology
Dalian, 116024, China

Abstract

The demand for high speed low resistance marine transportation for military, commercial, and recreational use is constantly increasing. Due to the ever rising prices of oil, it is of utmost importance to design ships that operate with a lower resistance at cruising speeds. Trimarans, which are classified as multi-hulled thin ships, are designed to meet the demand for high speeds while achieving a low resistance. This study focuses on the calculation of the frictional resistance of the trimaran hull form. A computation fluid dynamics program, *CFX 5.7*, was used to perform flow simulations on a computer generated model of a trimaran, in order to determine the frictional resistance of said trimaran. The numerical results were compared with an empirical formula in order to validate the *CFX* flow simulations. The numerical and empirical calculations proved to be dissimilar, resulting in unreliable estimations of the trimaran's frictional resistance.

Introduction

In today's economies time is a valuable commodity. The demand for faster modes of transportation, fuels the fields of research and engineering to develop solutions to these demands. Particular difficulty arises in the design of high speed ships. For marine vessels, as the speed increases, there is a relatively large increase in resistance to motion in the form of drag. The increase in drag therefore requires an increase in the power required to propel the ship, as well as the weight and size of the ship's engine. In order to meet the demands for high speed vessels, the field of Naval Architecture has begun testing many new ship forms. This paper is concerned with the study of the trimaran hull type configuration and hydrodynamics related to the trimaran; specifically

the frictional resistance of a trimaran. A list of symbols and abbreviations used in this paper can be found in Appendix A.

Background

A trimaran is a multi-hulled vessel, consisting of one long main hull and two shorter outriggers, also called wing hulls, located on both sides of the main hull; see Fig. 1.

Figure 1: Sail powered trimaran (Latitude 38 Publishing Co., Inc.)

The outriggers provide the trimaran with excellent stability and seakeeping characteristics (Kang et. al., 2001). A trimaran can be either wind driven as shown in Fig. 1, or mechanically driven. Another unique feature of the trimaran design is the small ratio of width to length. Trimarans are typically designed with very long and slender hull shapes in order to decrease the wave making resistance of the ship. The main hull and outriggers can also be arranged so that the waves produced by the ship destructively interfere, producing smaller waves and thereby losing less energy to wave-making resistance (Xu, H. and Zou, Z., 2001). Wave-making resistance is classified as the drag force on the trimaran which is created by the loss of energy to the formation of waves. The excellent seakeeping performance and the lower resistance at high speeds make the trimaran design appropriate for high speed travel applications.

Currently, trimarans are being used for business, recreation, and military applications because of their particular advantages over mono-hull ship designs. Trimarans have a much smaller draft than most boats, which allows them to access areas inaccessible to boats of similar size; draft is defined as the distance which a boat extends below the water surface. Ferries and sail boats have been designed using the trimaran configuration in order to provide the high speeds necessary for commercial transportation and racing. The trimaran design is also favorable for military and research applications due to the large open deck space available for equipment.

Much of the current information on trimarans comes from a study conducted by Britain's Defense Evaluation and Research Agency (*DERA*) along with the U.S. Navy. For the study, a two-thirds scale trimaran warship, called the *RV Triton* (see Fig. 2) was built to demonstrate the feasibility of the trimaran design for naval applications. The ship's length overall (*LOA*) was 95 *m*, weight 800 tonnes, and a draft of only 3 *m*.

Figure 2: RV Triton, trimaran design test ship (GlobalSecurity.org, 2006)

Studies performed by *DERA* on computer models and towing tank models showed that the trimaran configuration could reduce the overall drag of the ship by up to 20 percent, when compared to a mono-hull ship of similar size (Wilson, J. 1999). Similar research has been conducted on trimaran seakeeping performance and wave-making resistance using numerical models and towing tank tests (Kang, Xu, & Narita).

This study aims to determine the frictional resistance, R_F, of a trimaran by the use of a computer generated model. The frictional resistance of a ship is composed of the viscous resistance, R_V, and the form resistance, R_f. The viscous resistance is due to frictional forces resisting motion of the trimaran's hulls through the water. The form resistance, sometimes referred to as the viscous pressure resistance R_{VP}, is due to the pressure forces acting on the specific shape of the ship hulls. A body with a smaller cross-sectional area will tend to have less form drag. This is one of the reasons trimarans exhibit lower values of drag as compared to mono-hull ships.

In past research, numerical simulations have been performed to compute the wave-making resistance only, and drag results from towing tanks include the wave-making resistance component as well (Kang, Xu, & Narita). The frictional resistance however, is made up of only the viscous drag and form drag. In order to calculate the frictional resistance, computational fluid dynamics, *CFD*, software was used for the numerical simulation of the trimaran model and R_F calculation.

Methodology and Modeling

The numerical simulations in this study were performed on a trimaran with the station coordinates for the main hull and outriggers as shown in Tables 1 & 2.

Table 1: Main hull station coordinates (units mm)

Station #	0WL	400WL	800WL	1200WL	1600WL	1700WL
0	——	——	1700	1741	1782	1792
1	——	——	1700	1741	1782	1792
2	——	——	1700	1741	1782	1792
3	——	——	1700	1741	1782	1792
4	——	243	1700	1741	1782	1792
5	——	496	1700	1741	1782	1792
6	——	655	1700	1741	1782	1792
7	——	764	1694	1738	1779	1789
8	——	829	1662	1725	1766	1777
9	——	847	1594	1697	1741	1752
10	——	823	1496	1650	1699	1711
11	——	771	1371	1593	1656	1670
12	——	699	1228	1512	1600	1620
13	——	613	1075	1400	1515	1541
14	50	499	899	1219	1384	1419
15	49	393	728	999	1205	1247
16	44	301	568	791	983	1025
17	32	210	413	587	738	774
18	16	123	257	380	496	525
19	0	47	109	175	253	271
20	——	——	——	——	——	——

WL = verticle height of waterline

Table 2: Outrigger station coordinates (units mm)

Station #	0WL	200WL	400WL	600WL	800WL	1000WL
0	——	——	——	425	425	425
0.5	——	——	26	425	425	425
1	——	——	232	425	425	425
2	——	——	316	425	425	425
3	——	125	346	425	425	425
4	——	177	360	425	425	425
5	13	176	315	395	398	402
6	13	150	254	339	366	379
7	12	102	183	248	300	330
8	11	63	118	166	208	243
9		26	55	81	107	132
9.5	——	——	8	26	45	68
10	——	——	——	——	——	0

WL = verticle height of waterline

The resulting dimensions of the trimaran's main hull and outriggers, as derived from the station coordinates can be seen in Table 3.

Table 3: Trimaran dimensions

	Main Hull (m)	Outrigger (m)
Length	40	10
Breadth	3.6	0.9
Draft	1.7	1.0

The station coordinates shown in Tables 1 & 2 describe the trimaran's main hull and outriggers starting at the keel, and extending up to the design waterline, *DWL*, of the ship; Fig. 3 demonstrates the design scheme as described.

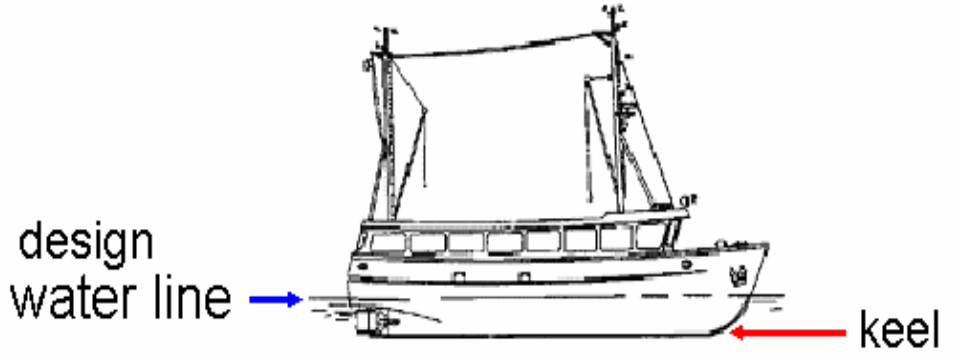

Figure 3: Design waterline and keel of ship (Baltija, 2006)

To begin the modeling process, the shape of the main hull was first drawn using *ANSYS 8.1 (ANSYS)*, see Figs, 4.a & 4.b.

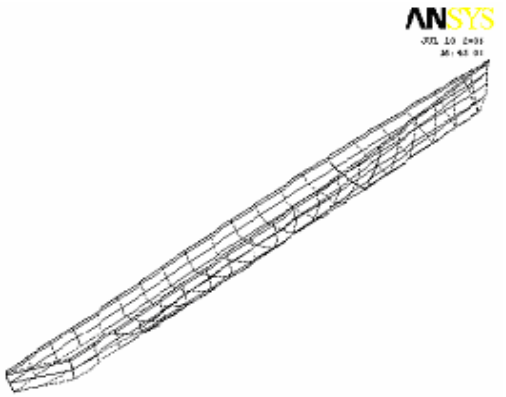

Figure 4.a: Lines for main hull, *ANSYS*

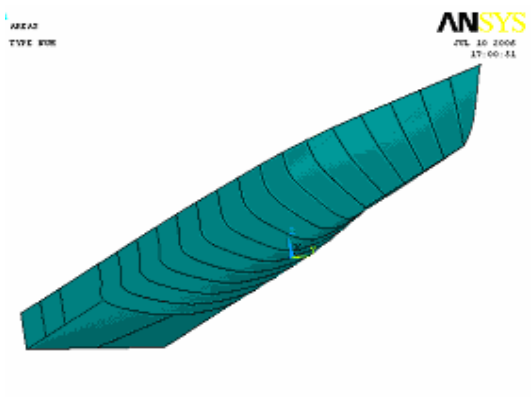

Figure 4.b: Areas for main hull, *ANSYS*

After drawing the main hull, the trimaran model was meshed with finite elements for use in the *CFD* analysis; see Fig. 5.

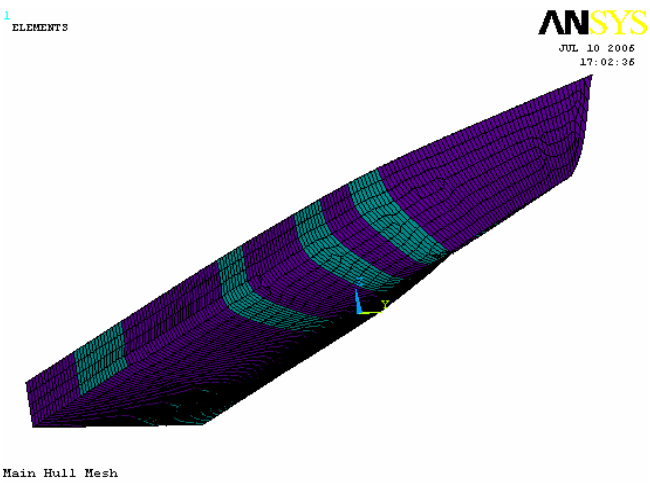

Figure 5: Mesh of main hull, *ANSYS*

It was soon discovered that one could not import a model meshed using *ANSYS* into *CFX 5.7 (CFX)*. Therefore, the model was drawn and meshed using a two part process.

The first step in the process was to draw the trimaran model using *Pro ENGINEER* (*ProE*). The model was then imported into *ANSYS ICEM 10.1(ICEM)* in order to create the finite element mesh and control volume necessary for use with *CFX*. At this time it was also necessary to make design changes to the trimaran's hull form; the current hull was much too round, as can be seen in the previous figures. High speed ships have hull forms with much sharper edges. Since, the trimaran is a high speed ship; this design change was taken into account when redrawing the trimaran using *ProE*. Figures 6.a & 6.b show the lines and areas used to draw the main hull and outriggers of the trimaran. The *ibl* files which were used to create the datum curves in *ProE* can be viewed in their entirety in Appendix B.

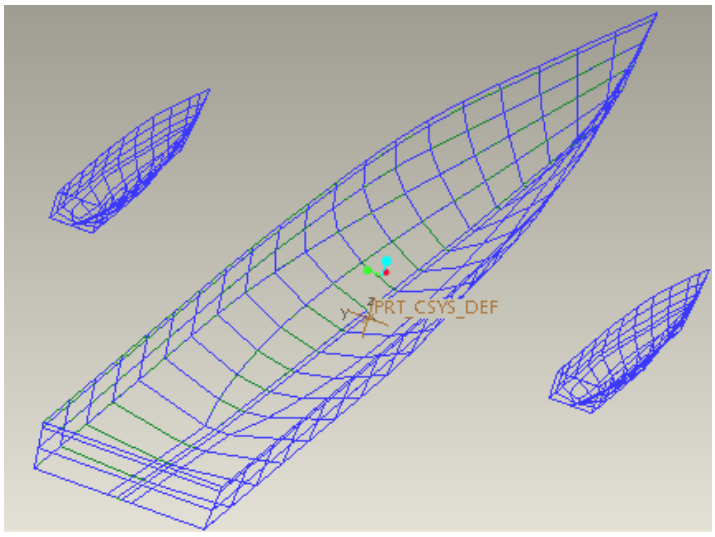

Figure 6.a: Lines creating main and wing hulls of trimaran, *ProE*

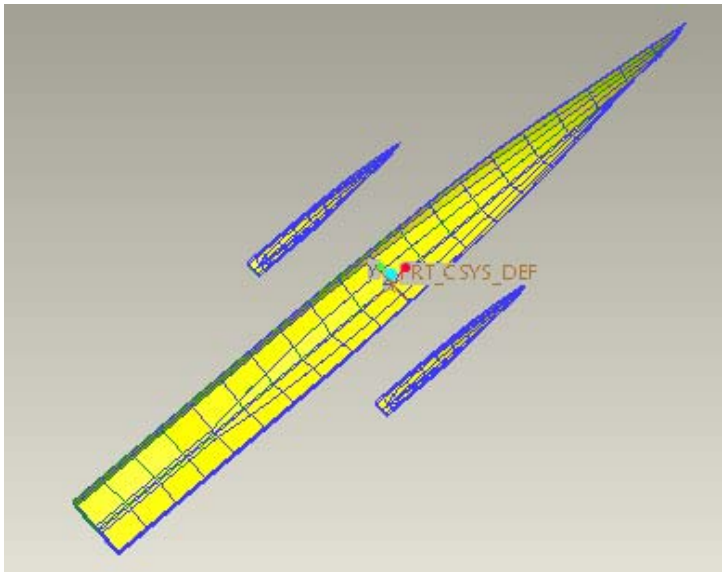

Figure 6.b: Areas creating main and wing hulls of trimaran, *ProE*

Following the completion of the *ProE* trimaran drawing, it was necessary to create a control volume and an element mesh on the trimaran for *CFD* analysis. *ICEM* was chosen to create the control volume for the simulation, as well as the mesh for the trimaran model because it was fully compatible with *CFX*. Once the model was loaded into *ICEM*, the control volume was created with the following dimensions: length 125 *m*, width 50 *m*, height 8.5 *m*. The trimaran was placed tangent to the top of the control volume, 5 *m* from the inlet, and centered relative to the sides. The control volume was made with these dimensions to ensure fully developed flow, and to be certain that the fluid/wall interactions of the control volume would not influence the frictional resistance calculations on the trimaran. The parts of the drawing were then labeled according to their purposes: inlet, outlet, top, bottom, side1, side2, and hull. The entire assembly was then meshed as seen in Fig. 7.

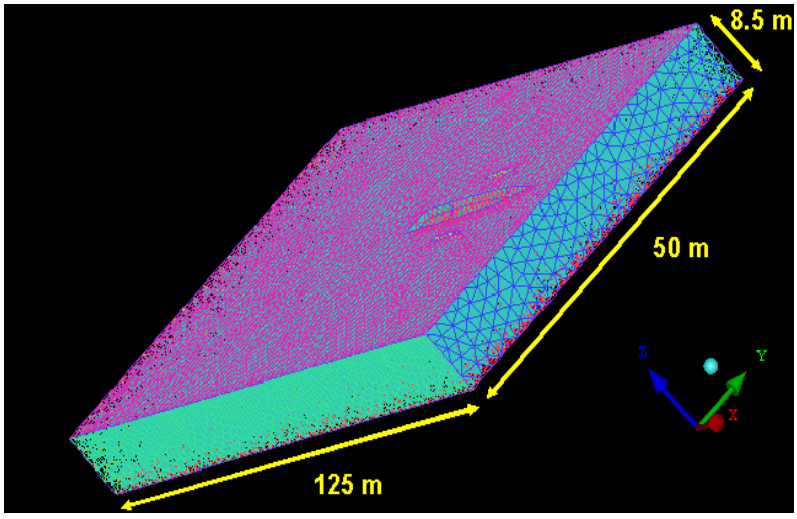

Figure 7: Meshed trimaran and control volume assembly, *ICEM*

Now that the assembly had been meshed, it was imported into *CFX* for *CFD* simulation and analysis. For all *CFX* simulations it is necessary to apply boundary conditions to all surfaces in the assembly. When applying boundary conditions, one must also specify the boundary type. The boundary conditions and types were applied to the control volume in the following order, name=type, to establish the physics of the model: inlet=INELT, outlet=OUTLET, top=wall, bottom=wall, side1=symmetry, side2=symmetry, and hull=wall; see Table 4.

Table 4: Description of boundary conditions applied to control volume surfaces

Surface Name	Boundary Condition Type
inlet	INLET
outlet	OUTLET
top	wall
bottom	wall
side1	symmetry
side 2	symmetry

Fig. 8 shows the completed *CFX* control volume, the inflow is indicated by the white arrows (right side of Fig. 8) and the outflow by the yellow arrows. With the boundary conditions and physical properties applied to the model, the initial simulation was begun.

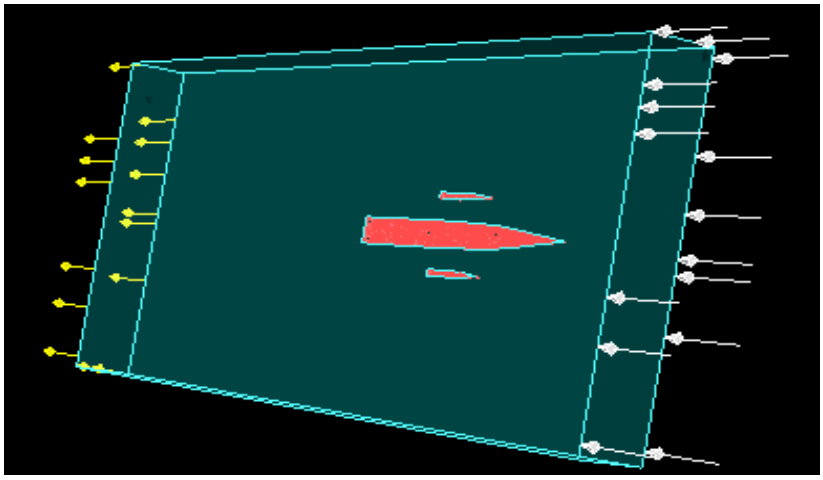

Figure 8: Assembly of control volume and trimaran, *CFX*

Having run the initial simulation, the results file was loaded into the post processor of the *CFX* program for further analysis. In order to determine the frictional resistance of the trimaran's hulls, the "function calculator" of the *CFX* post processor was used. The force on the trimaran was calculated and set equivalent to the frictional resistance, R_F. After the initial simulation at 2 *m/s*, additional simulations were run at speeds of 7, 10, 15, and 20 *m/s*. Data on the frictional resistance was gathered for the trimaran during each test.

With numerical values for the trimaran's frictional resistance established at varying

speeds, the results had to be checked versus an empirical formula to ensure the initial results obtained from the simulations were valid. The formula used for the empirical calculation of frictional resistance is shown in Eqn. 1 below.

$$R_F = C_F \left(\frac{1}{2} \rho V^2 \right) S \tag{1}$$

Where C_F is the coefficient of friction, ρ is the fluid density, V is the velocity, and S is the wetted surface area (Yanying, W. 2003). C_F was estimated using the, "International Towing Tank Conference (ITTC) 1957 model-ship correlation line" Eqn. (2) (Waters, J.K.).

$$C_F = \frac{0.075}{\left(\log_{10} R_n - 2 \right)^2} \tag{2}$$

In Eqn. (2), R_n is the Reynolds number, calculated using;

$$R_n = \frac{VL}{\nu} \tag{3}$$

The density, kinematic viscosity, and velocity were identical to the values used in the initial simulations, and were $998\, kg/m^3$, 10^{-6} m^2/s respectively; the velocity was varied in accordance with the initial simulations. The wetted surface area was calculated by first obtaining the analytical equations describing the curves of the trimaran's waterlines, from the keel to the *DWL*. The equations were then solved by Calculus integration techniques for the value of *S*. R_F values had to be calculated for both the main hull and outriggers, because the Reynolds number for each component differs due to their difference in length. The resultant empirical R_F values for the main hull and outriggers were then added together to obtain the frictional resistance of the entire trimaran, R_F. With both numerical and empirical results obtained, the two sets of data were compared in order to validate the results generated from the *CFX* simulations.

When the results from the numerical model and the empirical model were compared, it was apparent that there was a large difference in the calculated values for the frictional resistance of the trimaran. To correct for the difference in values, refinements were made to the computer generated trimaran model. The changes to the model included enhancement of the geometry to eliminate unnecessary lines and areas in the model, as well as the elimination of gaps and holes in the model. Once the geometry of the model was improved, the finite element mesh of the model was refined in *ICEM*. Refinements to the mesh included increasing the number of layers and elements on the trimaran hull, and the use of tetrahedral elements for the meshing process. After refining the trimaran model, numerical simulations were run again at velocities of 2, 7, 10, 15 and 20 *m/*s using *CFX*. Data on the trimaran's frictional resistance was gathered for each velocity tested and for each component hull of the trimaran.

Results

From the initial *CFX* simulation, the frictional resistance on the trimaran was calculated in the post processor using the "function calculator" for a speed of 2 *m/s*. The initial results showed that the frictional force was equal to 3,927.62 *N*. All of the numerical results for the simulations are compiled in Table 4.

Table 5: Initial numerical results for frictional resistance of trimaran

Velocity (m/s)	TOTAL R_F (N)
2	3927.62
7	48096.1
10	96995.2
15	215540.0
20	381642.0

The empirical value for the frictional resistance on the main hull and outriggers was calculated using Eqns 1-3. The component resistances of the main hull and outriggers were then added to obtain a R_F value for the entire trimaran. The resulting values derived from the use of Eqns. 1-3, for a velocity of 2 *m/s*, can be seen in Table 5.

Table 6: Empirical values for calculation of R_F at V=2 *m/s*

	Main Hull	Outrigger
S (m^2)	117.4985	8.024
R_n	8.00E+07	2.00E+07
C_F	0.00215	0.00267
R_F (N)	504.77	42.75
	TOTAL	590.26

A spreadsheet was then set up to calculate the empirical frictional resistance for velocities ranging from 0 to 20 *m/*s, in increments of 1 *m/*s. Figure 9 shows a graph of the empirical values; notice the data line shows the trend of increasing empirical resistance with increasing velocity for the trimaran model.

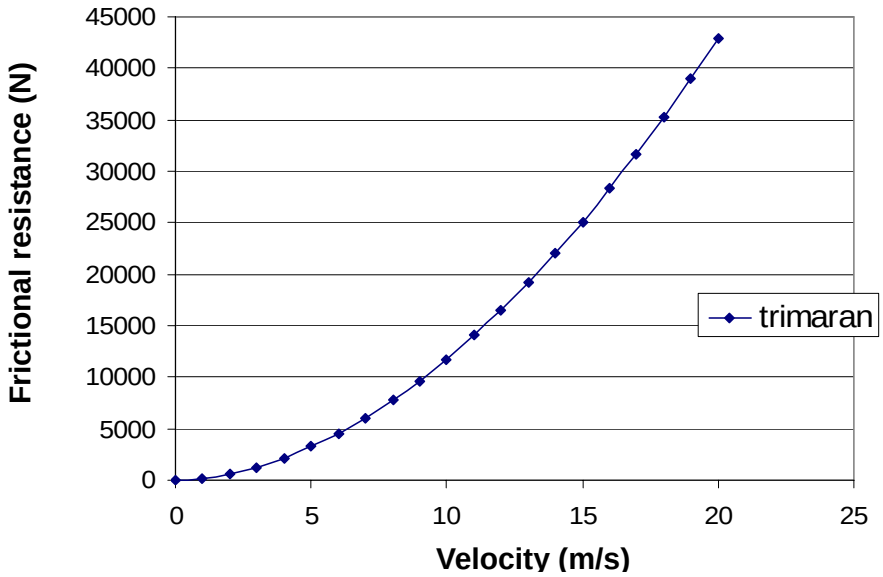

Figure 9: Empirical Data: R_F vs. Velocity

Upon comparing the numerical results from the initial *CFX* simulation with the empirical results, it was observed that there was a drastic difference in the R_F values; see Table 6 and Fig. 10.

Table 7: Comparison of initial numerical and empirical R_F values for trimaran

Velocity (m/s)	Total Initial Numerical R_F (N)	Total Empirical R_F (N)
2	3927.62	590.26
7	48096.1	6045.24
10	96995.2	11757.02
15	215540.0	25078.19
20	381642.0	42962.85

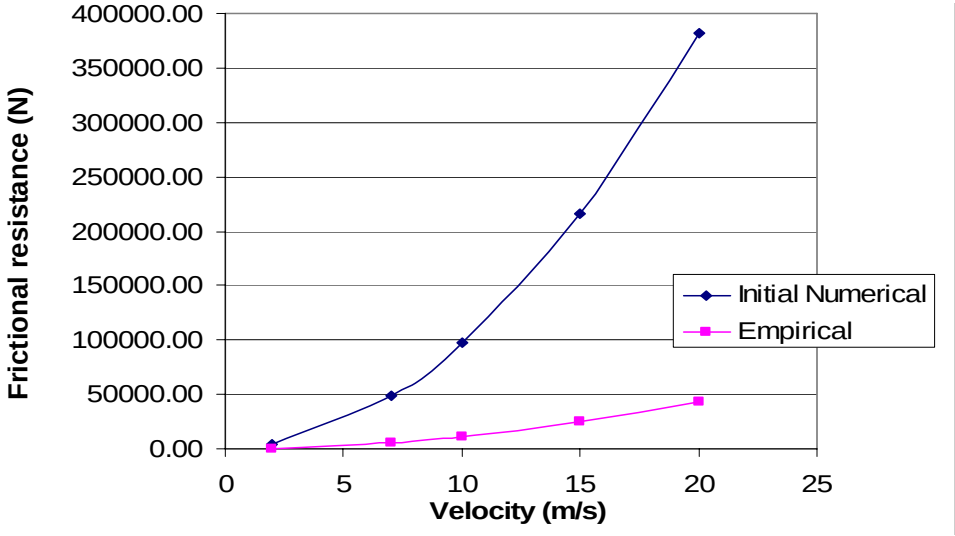

Figure 10: Initial numerical and empirical R_F data vs. velocity

An effort was made to improve the results obtained from the numerical simulation by refining the computer generated trimaran model. Refinements to the model included the elimination of holes in the geometry of the model, and enhancement of the model's finite element mesh. Figure 11 shows the improved *ICEM* mesh of the trimaran, notice the increased number of elements on the meshing of the trimaran in order to improve the computer's numerical iterations.

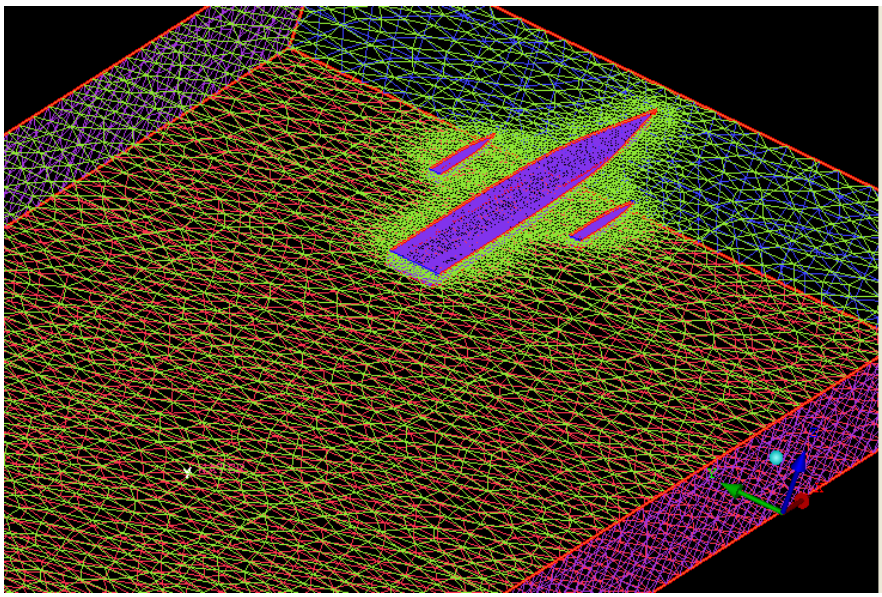

Figure 11: Refined finite element mesh, *ICEM*

From the *CFX* simulation of the refined trimaran model, the frictional resistance on each component hull of the trimaran was calculated in the post processor for a speed of

2 *m/s*. The results showed that the frictional force on the port-side (left) and starboard-side outriggers were equal to 509.34 *N* and 521.13 *N* respectively; while the force on the main hull was 2,706.07 *N*. Therefore the approximate numerical value of R_F for the refined model, as determined by the *CFX* simulation at a speed of 2 *m/s*, is equal to 3,736.5 *N*. The results obtained from the improved geometry for each velocity tested can be seen in Table 7.

Table 8: Numerical values of frictional resistance on refined trimaran model

Velocity (m/s)	Port-side Outrigger (N)	Starboard-side Outrigger (N)	MAIN HULL (N)	TOTAL refined R_F (N)
2	509.34	521.13	2706.07	3736.5
7	6026.46	6162.43	31407.5	43596.4
10	12194.40	12469.20	63188.0	87851.6
15	27199.70	27811.70	140097.0	195108.4
20	48074.30	49156.00	246596.0	343826.3

One will notice from Table 7 that the frictional resistance on the port and starboard outriggers is not of equal value. This is directly due to inconsistencies in the meshing process of *ICEM*, and was to be expected.

Although the values for the frictional resistance of the trimaran were lower for the refined model when compared to the initial simulations, the numerically calculated resistance was still much too large when compared to the empirical resistance. Figure 12 shows the similarity in the numerical results from the initial simulations and refined simulations.

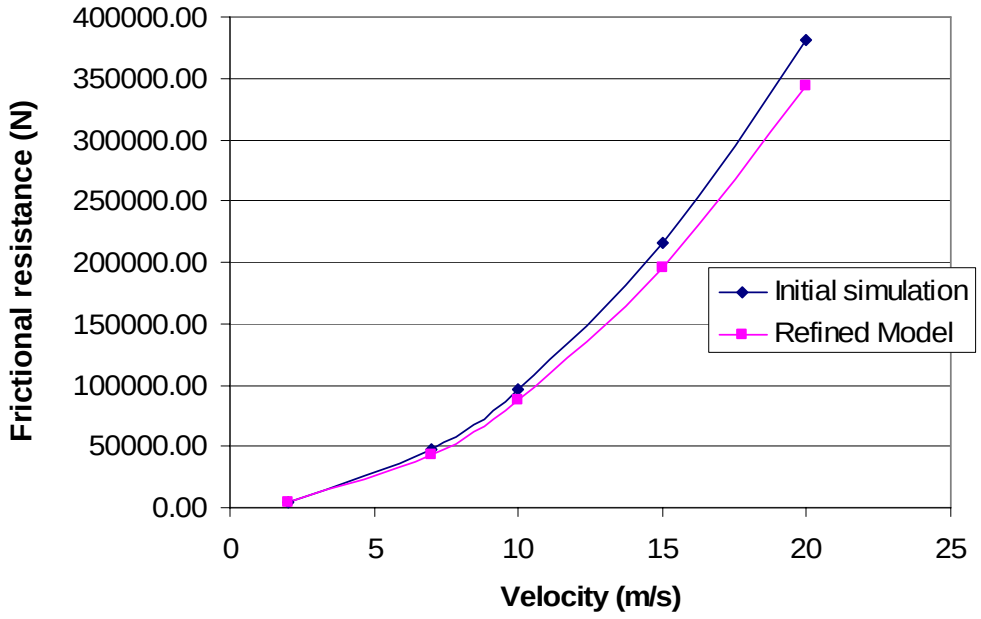

Figure 12: Comparison of initial and refined results for R_F *CFX* simulations

As Fig. 12 shows, the values for the frictional resistance of the trimaran during the

initial and refined simulations are of similar magnitude. However, the values for the numerical and empirical frictional resistance were still much different; see Table 8 and Fig. 13.

Table 9: Comparison of R_F values for the refined numerical simulations and the empirical calculations

Velocity (m/s)	Total Numerical R_F (N)	Total Empirical R_F (N)
2	3736.54	590.26
7	43596.39	6045.24
10	87851.60	11757.02
15	195108.40	25078.19
20	343826.30	42962.85

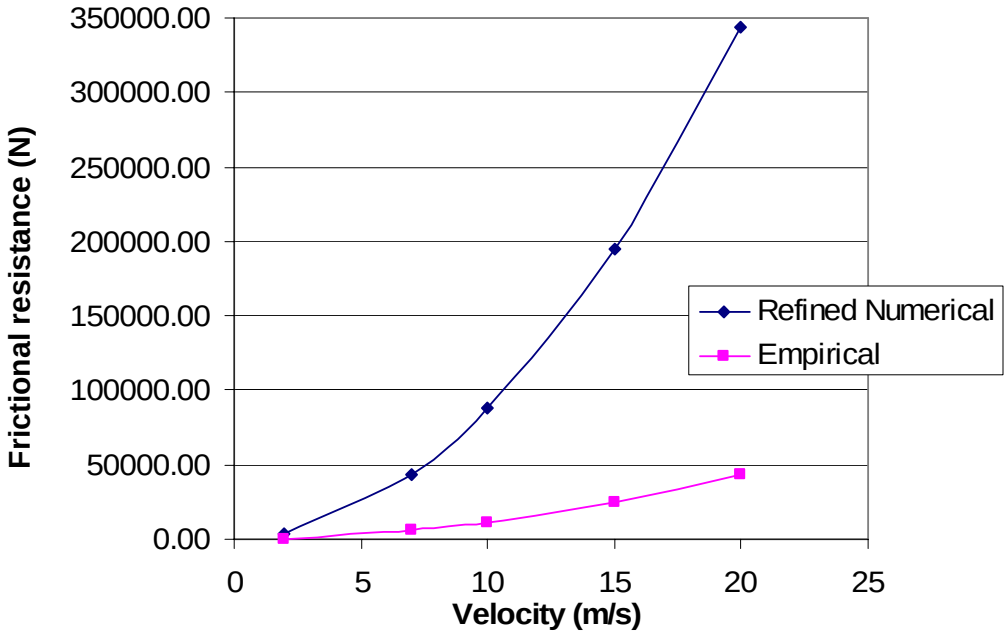

Figure 13: R_F data for refined numerical results and empirical results vs. velocity

As evident from Fig. 13, even with the refinement of the model, there was still a very large difference in the numerical and empirical results for the frictional resistance of the trimaran.

Conclusions & Recommendations

Due to the large magnitude of the difference between the numerical and empirical values for the frictional resistance, this study was unable to determine the frictional resistance of the trimaran hull form with any certainty. It is believed that the empirically calculated results for R_F hold more scientific value than the numerical

simulations. However, it is recommended that tests be performed on a scale model of the trimaran in a towing tank, in order to determine which, if any of the results from this study are correct. A test of this type would also enable one to pinpoint the source of error in the current study.

Acknowledgements

This material is based on work supported by the National Science Foundation under Grant No. OISE-0229657. Any opinions, findings, and conclusions expressed in this material are those of the author and do not necessarily reflect the views of the National Science Foundation.

References

Baltija Shipbuilding Yard, http://www.baltijos.lt/en/Products/type_fishing_boats_hulls.php, date visited: 06/04/2006

GlobalSecurity.org, http://www.globalsecurity.org/military/world/europe/triton.htm, date visited: 06/05/2006

Kang, K., et al. (2001) "Seakeeping and Maneuvering Performances of the 2,500 Tons Class Trimaran", *Proceedings of IWSH'2001 The Second International Workshop on Ship Hydrodynamics*, Wuhan, China, pp. 38-44

Latitude 38 Publishing Co., Inc., Sailing and Marine Magazine, http://www.latitude38.com/LectronicLat/2001/August2001/Aug30/trimaran.jpg, date visited: 07/10/2006

Marine Engineering World, http://www.free-marine.com/glossaryag.htm, date visited: 07/12/2006

Narita, S. (1976) "Some Research on the Wave Resistance of a Trimaran", *ISWR76*, pp. 381-388

Waters, J.K. (2004) *Principals of Ship Performance*, Naval Architecture and Ocean Engineering Department, U.S.N.A, Chapter 7 pp. 6-14, http://www.usna.edu

Wilson, J.(1999), "Sea Power 2000", *Popular Mechanics*, 1999, also available at: http://www.popularmechanics.com/science/defense/1281186.html date visited: 07/10/2006

Xu, H. and Zou, Z. (2001) "Numerical Prediction of Wavemaking Resistance of a Trimaran", *Proceedings of IWSH'2001 The Second International Workshop on Ship Hydrodynamics*, Wuhan, China, pp. 105-109

Yanying, W. (2003) *Ship Resistance*, Dalian University of Technology, China, pp. 7-11

Appendix A

Symbols & Abbreviations

Symbols & Abbreviations

CFX 5.7 ……..……*CFX*
LOA ……... Length Overall
m ……..meters
R_F …….……..... frictional resistance
R_V ……..….viscous resistance
R_f …….....form resistance
R_{VP} …….....viscous pressure resistance
kg …...…… kilogram
N …….. Newton
s ……seconds
ibl …….....file designation
L ……...length
CFD …Computational Fluid Dynamics
DWL ……...…Design Waterline
ANSYS 8.1 ……..*ANSYS*
Pro Engineer ……..…*ProE*
ANSYS ICEM 10.1 ……*ICEM*
C_F …….coefficient of friction
ρ ……..density
V ……....velocity
S ……...wetted surface area
R_n …….. Reynolds number
ν ……..….kinematic viscosity

Appendix B

ibl files for generation of ProE drawings

Main Hull Horizontal Coordinates

open
arclength
Begin section!
Begin curve!1
1 8 0.0500 0
2 10 0.0490 0
3 12 0.0440 0
4 14 0.0320 0
5 16 0.0160 0
6 18 0.0000 0
Begin curve!2
1 -12 0.2430 0.4
2 -10 0.4960 0.4
3 -8 0.6550 0.4
4 -6 0.7640 0.4
5 -4 0.8290 0.4
6 -2 0.8470 0.4
7 0 0.8230 0.4
8 2 0.7710 0.4
9 4 0.6990 0.4
10 6 0.6130 0.4
11 8 0.4990 0.4
Begin curve!3
1 8 0.4990 0.4
2 10 0.3930 0.4
3 12 0.3010 0.4
4 14 0.2100 0.4
5 16 0.1230 0.4
6 18 0.0470 0.4
7 18.965 0 0.4
Begin curve!4
1 -20 1.7000 0.8
2 -18 1.7000 0.8
3 -16 1.7000 0.8
4 -14 1.7000 0.8
5 -12 1.7000 0.8
Begin curve!5
1 -12 1.7000 0.8
2 -10 1.7000 0.8
3 -8 1.7000 0.8
4 -6 1.6940 0.8
5 -4 1.6620 0.8
6 -2 1.5940 0.8
7 0 1.4960 0.8
8 2 1.3710 0.8
9 4 1.2280 0.8
10 6 1.0750 0.8
11 8 0.8990 0.8
Begin curve!6
1 8 0.8990 0.8
2 10 0.7280 0.8
3 12 0.5680 0.8
4 14 0.4130 0.8
5 16 0.2570 0.8
6 18 0.1090 0.8
7 19.363 0 0.8
Begin curve!7
1 -20 1.7410 1.2
2 -18 1.7410 1.2
3 -16 1.7410 1.2
4 -14 1.7410 1.2

Main Hull Vertical Coordinates

open
arclength
Begin section!
Begin curve!1
-20 1.7000 0.8
-20 1.7410 1.2
Begin curve!2
-20 1.7410 1.2
-20 1.7820 1.6
Begin curve!3
-20 1.7820 1.6
-20 1.7920 1.7
Begin curve!4
-18 1.7000 0.8
-18 1.7410 1.2
Begin curve!5
-18 1.7410 1.2
-18 1.7820 1.6
Begin curve!6
-18 1.7820 1.6
-18 1.7920 1.7
Begin curve!7
-16 1.7000 0.8
-16 1.7410 1.2
Begin curve!8
-16 1.7410 1.2
-16 1.7820 1.6
Begin curve!9
-16 1.7820 1.6
-16 1.7920 1.7
Begin curve!10
-14 1.7000 0.8
-14 1.7410 1.2
Begin curve!11
-14 1.7410 1.2
-14 1.7820 1.6
Begin curve!12
-14 1.7820 1.6
-14 1.7920 1.7
Begin curve!13
-12 0.2430 0.4
-12 1.7000 0.8
Begin curve!14
-12 1.7000 0.8
-12 1.7410 1.2
Begin curve!15
-12 1.7410 1.2
-12 1.7820 1.6
Begin curve!16
-12 1.7820 1.6
-12 1.7920 1.7
Begin curve!17
-10 0.4960 0.4
-10 1.7000 0.8
Begin curve!18
-10 1.7000 0.8
-10 1.7410 1.2
Begin curve!19
-10 1.7410 1.2
-10 1.7820 1.6
Begin curve!20
-10 1.7820 1.6

5 -12 1.7410 1.2
Begin curve!8
1 -12 1.7410 1.2
2 -10 1.7410 1.2
3 -8 1.7410 1.2
4 -6 1.7380 1.2
5 -4 1.7250 1.2
6 -2 1.6970 1.2
7 0 1.6500 1.2
8 2 1.5930 1.2
9 4 1.5120 1.2
10 6 1.4000 1.2
11 8 1.2190 1.2
Begin curve!9
1 8 1.2190 1.2
2 10 0.9990 1.2
3 12 0.7910 1.2
4 14 0.5870 1.2
5 16 0.3800 1.2
6 18 0.1750 1.2
7 19.667 0 1.2
Begin curve!10
1 -20 1.7820 1.6
2 -18 1.7820 1.6
3 -16 1.7820 1.6
4 -14 1.7820 1.6
5 -12 1.7820 1.6
Begin curve!11
1 -12 1.7820 1.6
2 -10 1.7820 1.6
3 -8 1.7820 1.6
4 -6 1.7790 1.6
5 -4 1.7660 1.6
6 -2 1.7410 1.6
7 0 1.6990 1.6
8 2 1.6560 1.6
9 4 1.6000 1.6
10 6 1.5150 1.6
11 8 1.3840 1.6
Begin curve!12
1 8 1.3840 1.6
2 10 1.2050 1.6
3 12 0.9830 1.6
4 14 0.7380 1.6
5 16 0.4960 1.6
6 18 0.2530 1.6
7 19.935 0 1.6
Begin curve!13
1 -20 1.7920 1.7
2 -18 1.7920 1.7
3 -16 1.7920 1.7
4 -14 1.7920 1.7
5 -12 1.7920 1.7
Begin curve!14
1 -12 1.7920 1.7
2 -10 1.7920 1.7
3 -8 1.7920 1.7
4 -6 1.7890 1.7
5 -4 1.7770 1.7
6 -2 1.7520 1.7
7 0 1.7110 1.7

-10 1.7920 1.7
Begin curve!21
-8 0.6550 0.4
-8 1.7000 0.8
Begin curve!22
-8 1.7000 0.8
-8 1.7410 1.2
Begin curve!23
-8 1.7410 1.2
-8 1.7820 1.6
Begin curve!24
-8 1.7820 1.6
-8 1.7920 1.7
Begin curve!25
-6 0.7640 0.4
-6 1.6940 0.8
Begin curve!26
-6 1.6940 0.8
-6 1.7380 1.2
Begin curve!27
-6 1.7380 1.2
-6 1.7790 1.6
Begin curve!28
-6 1.7790 1.6
-6 1.7890 1.7
Begin curve!29
-4 0.8290 0.4
-4 1.6620 0.8
Begin curve!30
-4 1.6620 0.8
-4 1.7250 1.2
Begin curve!31
-4 1.7250 1.2
-4 1.7660 1.6
Begin curve!
-4 1.7660 1.6
-4 1.7770 1.7
Begin curve!32
-2 0.8470 0.4
-2 1.5940 0.8
Begin curve!33
-2 1.5940 0.8
-2 1.6970 1.2
Begin curve!34
-2 1.6970 1.2
-2 1.7410 1.6
Begin curve!35
-2 1.7410 1.6
-2 1.7520 1.7
Begin curve!36
0 0.8230 0.4
0 1.4960 0.8
Begin curve!37
0 1.4960 0.8
0 1.6500 1.2
Begin curve!38
0 1.6500 1.2
0 1.6990 1.6
Begin curve!39
0 1.6990 1.6
0 1.7110 1.7
Begin curve!40
2 0.7710 0.4

8 2 1.6700 1.7
9 4 1.6200 1.7
10 6 1.5410 1.7
11 8 1.4190 1.7

Begin curve!15
1 8 1.4190 1.7
2 10 1.2470 1.7
3 12 1.0250 1.7
4 14 0.7740 1.7
5 16 0.5250 1.7
6 18 0.2710 1.7
7 20.125 0 1.7

Begin curve!16
1 8 0.0500 0
2 8 0.4990 0.4

Begin curve!17
1 8 0.4990 0.4
2 8 0.8990 0.8
3 8 1.2190 1.2
4 8 1.3840 1.6
5 8 1.4190 1.7

Begin curve!18
1 -12 0.2430 0.4
2 -12 1.7000 0.8

Begin curve!19
1 -12 1.7000 0.8
2 -12 1.7410 1.2
3 -12 1.7820 1.6
4 -12 1.7920 1.7

Begin curve!20
1 -20 1.7000 0.8
2 -20 0 0.8

Begin curve!21
1 -20 1.7410 1.2
2 -20 0 1.2
Begin curve!22
1 -20 1.7820 1.6
2 -20 0 1.6
Begin curve!23
1 -20 1.7920 1.7
2 -20 0 1.7
Begin curve!24
1 -12 0.2430 0.4
2 -12 0.05 0.4
Begin curve!25
1 8 0.0500 0
2 8 0 0
Begin curve!26
1 18 0 0.0
2 18.965 0 0.4
3 19.363 0 0.8
4 19.667 0 1.2
5 19.935 0 1.6
6 20.125 0 1.7

Begin curve!27
1 -12 0.05 0.4
2 -20 0.05 0.8

Begin curve!28
1 -12 0.05 0.4
2 -12 0.00 0.4

2 1.3710 0.8
Begin curve!41
2 1.3710 0.8
2 1.5930 1.2
Begin curve!42
2 1.5930 1.2
2 1.6560 1.6
Begin curve!43
2 1.6560 1.6
2 1.6700 1.7

Begin curve!44
4 0.6990 0.4
4 1.2280 0.8
Begin curve!45
4 1.2280 0.8
4 1.5120 1.2
Begin curve!46
4 1.5120 1.2
4 1.6000 1.6
Begin curve!47
4 1.6000 1.6
4 1.6200 1.7

Begin curve!48
6 0.6130 0.4
6 1.0750 0.8
Begin curve!49
6 1.0750 0.8
6 1.4000 1.2
Begin curve!50
6 1.4000 1.2
6 1.5150 1.6
Begin curve!51
6 1.5150 1.6
6 1.5410 1.7

Begin curve!52
8 0 0
8 0.0500 0
Begin curve!53
8 0.0500 0
8 0.4990 0.4
Begin curve!54
8 0.4990 0.4
8 0.8990 0.8
Begin curve!55
8 0.8990 0.8
8 1.2190 1.2
Begin curve!56
8 1.2190 1.2
8 1.3840 1.6
Begin curve!57
8 1.3840 1.6
8 1.4190 1.7

Begin curve!58
10 0.0490 0
10 0.3930 0.4
Begin curve!59
10 0.3930 0.4
10 0.7280 0.8
Begin curve!60
10 0.7280 0.8
10 0.9990 1.2
Begin curve!61
10 0.9990 1.2
10 1.2050 1.6
Begin curve!62

Begin curve!29
1 8 0.05 0.0
2 -12 0.05 0.4

Wing Hull Coordinates

open
arclength
Begin section!
Begin curve!1
-5 0.0125 0.4710
-5 0.4250 0.4710
Begin curve!2
-5 0.4250 0.4710
-5 0.4250 1.0000
Begin curve!2
-4.5 0.0125 0.4
-4.5 0.4250 0.4700
Begin curve!4
-4.5 0.4250 0.4700
-4.5 0.4250 0.6000
Begin curve!5
-4.5 0.4250 0.6000
-4.5 0.4250 0.8000
Begin curve!6
-4.5 0.4250 0.8000
-4.5 0.4250 1.0000
Begin curve!7
-4 0.0125 0.3280
-4 0.2320 0.4000
Begin curve!8
-4 0.2320 0.4000
-4 0.4250 0.4700
Begin curve!9
-4 0.4250 0.4700
-4 0.4250 0.6000
Begin curve!10
-4 0.4250 0.6000
-4 0.4250 0.8000
Begin curve!11
-4 0.4250 0.8000
-4 0.4250 1.0000
Begin curve!12
-3 0.0125 0.2000
-3 0.3160 0.4000
Begin curve!13
-3 0.3160 0.4000
-3 0.4250 0.4700
Begin curve!14
-3 0.4250 0.4700
-3 0.4250 0.6000
Begin curve!15
-3 0.4250 0.6000
-3 0.4250 0.8000
Begin curve!16
-3 0.4250 0.8000
-3 0.4250 1.0000
Begin curve!17
-2 0.0125 0.0990
-2 0.1250 0.2000

10 1.2050 1.6
10 1.2470 1.7
Begin curve!63
12 0.0440 0
12 0.3010 0.4
Begin curve!64
12 0.3010 0.4
12 0.5680 0.8
Begin curve!65
12 0.5680 0.8
12 0.7910 1.2
Begin curve!66
12 0.7910 1.2
12 0.9830 1.6
Begin curve!67
12 0.9830 1.6
12 1.0250 1.7
Begin curve!68
14 0.0320 0
14 0.2100 0.4
Begin curve!69
14 0.2100 0.4
14 0.4130 0.8
Begin curve!70
14 0.4130 0.8
14 0.5870 1.2
Begin curve!71
14 0.5870 1.2
14 0.7380 1.6
Begin curve!72
14 0.7380 1.6
14 0.7740 1.7
Begin curve!73
16 0.0160 0
16 0.1230 0.4
Begin curve!74
16 0.1230 0.4
16 0.2570 0.8
Begin curve!75
16 0.2570 0.8
16 0.3800 1.2
Begin curve!76
16 0.3800 1.2
16 0.4960 1.6
Begin curve!77
16 0.4960 1.6
16 0.5250 1.7
Begin curve!78
18 0.0000 0
18 0.0470 0.4
Begin curve!79
18 0.0470 0.4
18 0.1090 0.8
Begin curve!80
18 0.1090 0.8
18 0.1750 1.2
Begin curve!81
18 0.1750 1.2
18 0.2530 1.6
Begin curve!82
18 0.2530 1.6
18 0.2710 1.7
Begin curve!83
18.965 0 0.4

Begin curve!18		
-2	0.1250	0.2000
-2	0.3460	0.4000
Begin curve!19		
-2	0.3460	0.4000
-2	0.4250	0.4700
Begin curve!20		
-2	0.4250	0.4700
-2	0.4250	0.6000
Begin curve!21		
-2	0.4250	0.6000
-2	0.4250	0.8000
Begin curve!22		
-2	0.4250	0.8000
-2	0.4250	1.0000
Begin curve!23		
-1	0.0125	0.0210
-1	0.1770	0.2000
Begin curve!24		
-1	0.1770	0.2000
-1	0.3600	0.4000
Begin curve!25		
-1	0.3600	0.4000
-1	0.4250	0.4700
Begin curve!26		
-1	0.4250	0.4700
-1	0.4250	0.6000
Begin curve!27		
-1	0.4250	0.6000
-1	0.4250	0.8000
Begin curve!28		
-1	0.4250	0.8000
-1	0.4250	1.0000
Begin curve!29		
0	0.0125	0.0000
0	0.1760	0.2000
Begin curve!30		
0	0.1760	0.2000
0	0.3150	0.4000
Begin curve!31		
0	0.3150	0.4000
0	0.3590	0.4700
Begin curve!32		
0	0.3590	0.4700
0	0.3950	0.6000
Begin curve!33		
0	0.3950	0.6000
0	0.3980	0.8000
Begin curve!34		
0	0.3980	0.8000
0	0.4020	1.0000
Begin curve!35		
1	0.0125	0.0000
1	0.1500	0.2000
Begin curve!36		
1	0.1500	0.2000
1	0.2540	0.4000
Begin curve!37		
1	0.2540	0.4000
1	0.2860	0.4700
Begin curve!38		
1	0.2860	0.4700
1	0.3390	0.6000
Begin curve!39		
1	0.3390	0.6000
1	0.3660	0.8000

19.363	0	0.8
Begin curve!84		
19.363	0	0.8
19.667	0	1.2
Begin curve!85		
19.667	0	1.2
19.935	0	1.6
Begin curve!86		
19.935	0	1.6
20.125	0	1.7

Begin curve!40		
1	0.3660	0.8000
1	0.3790	1.0000
Begin curve!41		
2	0.0125	0.0000
2	0.1020	0.2000
Begin curve!42		
2	0.1020	0.2000
2	0.1830	0.4000
Begin curve!43		
2	0.1830	0.4000
2	0.2080	0.4700
Begin curve!44		
2	0.2080	0.4700
2	0.2480	0.6000
Begin curve!45		
2	0.2480	0.6000
2	0.3000	0.8000
Begin curve!46		
2	0.3000	0.8000
2	0.3300	1.0000
Begin curve!47		
3	0.0110	0.0000
3	0.0630	0.2000
Begin curve!48		
3	0.0630	0.2000
3	0.1180	0.4000
Begin curve!49		
3	0.1180	0.4000
3	0.1360	0.4700
Begin curve!47		
3	0.1360	0.4700
3	0.1660	0.6000
Begin curve!51		
3	0.1660	0.6000
3	0.2080	0.8000
Begin curve!52		
3	0.2080	0.8000
3	0.2430	1.0000
Begin curve!53		
4	0	0
4	0.0260	0.2000
Begin curve!54		
4	0.0260	0.2000
4	0.0550	0.4000
Begin curve!55		
4	0.0550	0.4000
4	0.0640	0.4700
Begin curve!54		
4	0.0640	0.4700
4	0.0810	0.6000
Begin curve!57		
4	0.0810	0.6000
4	0.1070	0.8000
Begin curve!58		
4	0.1070	0.8000
4	0.1320	1.0000
Begin curve!59		
4.5	0.0000	0.4000
4.5	0.0680	1.0000
Begin curve!64		
-5	0.4250	1.0
-4.5	0.4250	1.0
-4	0.4250	1.0

-3	0.4250	1.0
-2	0.4250	1.0
-1	0.4250	1.0
0	0.4020	1.0
1	0.3790	1.0
2	0.3300	1.0
3	0.2430	1.0
4	0.1320	1.0
Begin curve!65		
4	0.132	1.0
4.5	0.0680	1.0
Begin curve!66		
4.5	0.068	1.0
5	0.0000	1.0
Begin curve!65		
-5	0.0125	0.471
-4.5	0.0125	0.4
-4	0.0125	0.328
-3	0.0125	0.2
-2	0.0125	0.099
Begin curve!66		
-2	0.0125	0.099
-1	0.0125	0.021
0	0.0125	0
1	0.0125	0.0000
2	0.0125	0.0000
Begin curve!67		
2	0.0125	0.0000
3	0.0110	0.0000
4	0	0
Begin curve!66		
-5	0.4250	1.0
-5	0.0000	1.0
Begin curve!67		
4	0	0
4.5	0.0000	0.4000
Begin curve!68		
4.5	0.0000	0.4000
5	0.0000	1.0
Begin curve!68		
-4.5	0.0125	0.4
-4	0.2320	0.4000
-3	0.3160	0.4000
-2	0.3460	0.4000
-1	0.3600	0.4000
0	0.3150	0.4000
1	0.2540	0.4000
2	0.1830	0.4000
3	0.1180	0.4000
4	0.0550	0.4000
Begin curve!69		
4	0.0550	0.4000
4.5	0.0000	0.4000
Begin curve!69		
-5	0.0000	0.4710
-5	0.0125	0.4710
Begin curve!70		
-2	0.0000	0.0990
-2	0.0125	0.0990
Begin curve!71		
2	0.0000	0.0000
2	0.0125	0.0000